Localization of Charged Objects Using a Planar Electrostatic Sensor Array

Yonghui Hu, *Senior Member*, *IEEE*, Junkai Wang, Yi Li, Yong Yan, *Fellow*, *IEEE*

***Abstract*—Localization of charged objects is of great interest in a diverse range of industrial, commercial and military applications. This paper presents a method for locating charged objects in a plane using an electrostatic sensor array. Based on a simplified analytical model of the electrostatic sensor embedded in a grounded surface, a closed-form solution to the localization problem is derived for a linear sensor array, while the Newton-Raphson numerical method is used to approximate the solution for three randomly positioned sensors. Numerical simulations show that the charged object can be accurately located using the linear sensor array in areas far from the electrodes and the grounded surface. Depending on the initial value, the numerical solution for randomly positioned sensors may converge to correct or incorrect results and may diverge as well.**

***Index Terms*—Localization, charged object, electrostatic sensor, point charge, analytical model, numerical solution.**

I. Introduction

ELECTROSTATIC sensors have been used extensively to monitor the motion of charged objects [1], such as solid particles in pneumatic conveying pipelines, mechanical components in rotating machinery and human bodies performing daily activities. Various quantities regarding the motion state of objects have been inferred from induced electrostatic signals. On many occasions, it is important to know the location of a charged object. For instance, the indoor location of elderly people who are naturally, triboelectrically charged plays a vital role in Ambient Assisted Living (AAL) systems [2].

A few previous studies have proven the feasibility of locating a charged object using an array of electrostatic sensors. Trinks and Haseborg [3] placed three plate sensors at the corners of a triangle on the Earth surface to determine the path, velocity and altitude of an aircraft hundreds of meters away. A network of solid-state electric field sensors and the triangulation algorithm were used by Noras *et al*. to detect the trajectory of a bullet [4]. Addabbo *et al.* [5] estimated the trajectory position, charge and velocity of a debris particle in an exhaust conduit using two or three electrostatic sensors by combining the physical model and geometrical characteristics of the sensor array. In order to locate an aerial target generating an AC electric field, Zhang *et al*. [6] developed a mathematical model of the target location using a circular array of disk-shaped electric field sensors. Localization of human subjects through electric potential measurement has been investigated using sensor arrays in different configurations, i.e. four sensors positioned at the corners of a 5 m × 5 m square area [7], six ceiling-mounted sensors arranged at the corners of two rectangular cells covering an area of 2 m × 2.5 m [8], and a grid of electrode wires deployed underneath a non-conductive floor [9].

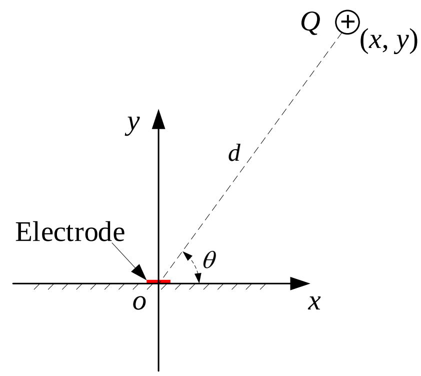

Fig. 1. Model of the electrostatic sensor.

Localization of a charged object using electrostatic sensors at known locations is an inverse problem. Generally, it is very difficult, if not impossible, to find a solution due to the complex spatial distribution of the electric field. In this paper, it is demonstrated for the first time that an analytical or numerical solution exists for a planar localization problem with appropriate simplifications. A variety of localization problems can be formulated in a plane, such as positioning of debris particles and bullets in the sensor plane, indoor human localization, and positioning of roping flow in the cross-section of a pneumatic conduit. A detailed derivation of the solution is presented and its validity verified numerically in this paper.

II. Mathematical Model and Localization Method

A. A Simplified Analytic Model of Electrostatic Sensors

For the planar localization problem, it is assumed that the distance between the charged object and the electrostatic sensor is much larger than the dimensions of the electrode and the charged object. As a result, the charged object can be modelled as a point charge and the electric field on the electrode surface regarded to be uniform. In some real scenarios, it might be more

Manuscript received Month xx, 20xx; revised Month xx, 20xx; accepted Month xx, 20xx. This work was supported by the National Natural Science Foundation of China under Grant 61973115. (*Corresponding author: Yonghui Hu*)

Y. Hu, J. Wang and Y. Li are with the School of Control and Computer Engineering, North China Electric Power University, Beijing 102206, China (phone: 86-10-61771330; e-mail: huyhui@gmail.com).

Y. Yan is with the School of Engineering, University of Kent, Canterbury, Kent CT2 7NT, UK (e-mail: y.yan@kent.ac.uk).

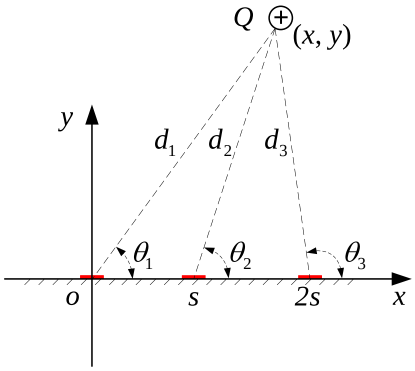

Fig. 2. Localization using a linear sensor array.

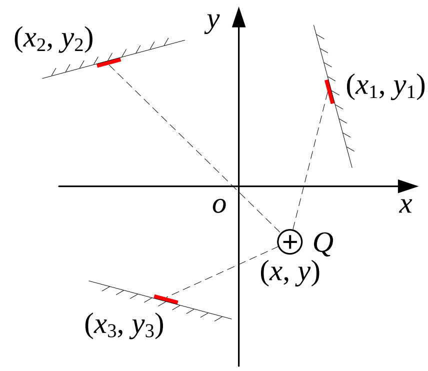

Fig. 3. Localization using three randomly positioned sensors.

appropriate to model the charged object as a line charge. In this case, the idea of planar localization presented is still viable with some modifications to the equations. As shown in Fig. 1, the electrode surface is perpendicular to the localization plane, on which the point charge and the center of the electrode are located. In addition, the electrode is embedded in a grounded surface of infinite size, which is in practice the masonry or concrete wall for indoor human localization or the metallic pipe wall for particle localization.

Using the method of images, the normal electric field $E_\perp$ at the center of the electrode is expressed as [10]

$$E_\perp = \frac{Q}{2\pi\varepsilon d^2}\sin\theta \tag{1}$$

where Q is the quantity of the point charge, ε is the permittivity of the medium, d is the distance between the point charge and the center of the electrode, and θ is the angle between the positive x-axis and the line connecting the center of the electrode and the point charge. According to the Gauss law, the total induced charge on the electrode is given by

$$\begin{aligned} Q' &= -\varepsilon E_\perp A \\ &= -\frac{AQ}{2\pi d^2}\sin\theta \end{aligned} \tag{2}$$

where A is the area of the electrode surface.

B. Localization Using a Linear Sensor Array

Because the quantity of the point charge is unknown and usually stochastic in practice, the absolute value of the induced charge cannot be used for localization. Instead, the relative magnitudes of the induced charges on the three electrodes are used to determine the coordinates of the point charge. As shown in Fig. 2, the three sensors numbered using i=1, 2 and 3 are placed in a linear array and evenly spaced. From equation (2), it is known that the induced charge on the i-th electrode is expressed as

$$Q_i' = -\frac{AQ}{2\pi d_i^2}\sin\theta_i \tag{3}$$

The relative magnitude of the induced charges is calculated as

$$\frac{Q_i'}{Q_j'} = \frac{d_j^2 \sin\theta_i}{d_i^2 \sin\theta_j} \tag{4}$$

where j=1, 2 and 3, and $i \neq j$. From the law of Sines in trigonometry, we obtain

$$\frac{d_i}{\sin\theta_j} = \frac{d_j}{\sin\theta_i} \tag{5}$$

Substituting equation (5) into (4) yields

$$\frac{Q_i'}{Q_j'} = \frac{\sin^3\theta_i}{\sin^3\theta_j} \tag{6}$$

According to Apollonius theorem, the following relationship holds:

$$d_1^2 + d_3^2 = 2s^2 + 2d_2^2 \tag{7}$$

where s is the center-to-center spacing between adjacent electrodes. Substituting equation (5) into (7) yields

$$\begin{cases} d_1^2 + \dfrac{\sin^2\theta_1}{\sin^2\theta_3} d_1^2 = 2s^2 + 2\dfrac{\sin^2\theta_1}{\sin^2\theta_2} d_1^2 \\ \dfrac{\sin^2\theta_3}{\sin^2\theta_1} d_3^2 + d_3^2 = 2s^2 + 2\dfrac{\sin^2\theta_3}{\sin^2\theta_2} d_3^2 \end{cases} \tag{8}$$

By substituting (6) into (8), the distances d_1 and d_3 are solved as

$$\begin{cases} d_1 = \dfrac{\sqrt{2}s}{\left[1 + \left(\dfrac{Q_1'}{Q_3'}\right)^{\frac{2}{3}} - 2\left(\dfrac{Q_1'}{Q_2'}\right)^{\frac{2}{3}}\right]^{\frac{1}{2}}} \\ d_3 = \dfrac{\sqrt{2}s}{\left[1 + \left(\dfrac{Q_3'}{Q_1'}\right)^{\frac{2}{3}} - 2\left(\dfrac{Q_3'}{Q_2'}\right)^{\frac{2}{3}}\right]^{\frac{1}{2}}} \end{cases} \tag{9}$$

Using the law of Cosines, the angle θ_1 is calculated as

$$\theta_1 = \arccos\frac{d_1^2 + 4s^2 - d_3^2}{4d_1 s} \tag{10}$$

Once d_1 and θ_1 are obtained, the coordinates of the point charge Q are found. The above derivation illustrates that it is feasible to determine the location of the point charge analytically using the relative magnitudes of the induced charges on the three linearly arranged electrodes.

C. Localization Using Three Randomly Positioned Sensors

In principle, the location of the point charge can be determined using three randomly positioned electrostatic sensors, as long as the point charge locates within the area enclosed by the three grounded surfaces. In this sense, the linear sensor array presented above is a special case. Since analytical solutions do not exist for arbitrary sensor locations, a numerical method is resorted to find a solution to the localization problem.

Without loss of generality, suppose the center of the *i*-th electrode is located at (x_i, y_i), as shown in Fig. 3. Then the grounded surface in the plane is described by

$$k_i(x-x_i)-(y-y_i)=0 \tag{11}$$

where k_i is the slope of the grounded surface. Then the distance from the point charge located at (x, y) to the grounded surface is calculated as

$$l_i=\frac{|k_i x-y-k_i x_i+y_i|}{(1+k_i^2)^{\frac{1}{2}}} \tag{12}$$

Based on equation (2), the induced charge on the *i*-th electrode is given by

$$\begin{aligned} Q_i' &= -\frac{AQl_i}{2\pi d_i^3} \\ &= -\frac{AQ|k_i x-y-k_i x_i+y_i|}{2\pi[(x-x_i)^2+(y-y_i)^2]^{\frac{3}{2}}(1+k_i^2)^{\frac{1}{2}}} \end{aligned} \tag{13}$$

Then the relative magnitudes of the induced charges on the electrodes are calculated as

$$\begin{cases} \dfrac{Q_1'}{Q_2'}=\dfrac{|k_1x-y-k_1x_1+y_1|[(x-x_2)^2+(y-y_2)^2]^{\frac{3}{2}}(1+k_2^2)^{\frac{1}{2}}}{|k_2x-y-k_2x_2+y_2|[(x-x_1)^2+(y-y_1)^2]^{\frac{3}{2}}(1+k_1^2)^{\frac{1}{2}}} \\ \dfrac{Q_1'}{Q_3'}=\dfrac{|k_1x-y-k_1x_1+y_1|[(x-x_3)^2+(y-y_3)^2]^{\frac{3}{2}}(1+k_3^2)^{\frac{1}{2}}}{|k_3x-y-k_3x_3+y_3|[(x-x_1)^2+(y-y_1)^2]^{\frac{3}{2}}(1+k_1^2)^{\frac{1}{2}}} \end{cases} \tag{14}$$

Equation (14) is rewritten as

$$\begin{cases} Q_1'|k_2x-y-k_2x_2+y_2|[(x-x_1)^2+(y-y_1)^2]^{\frac{3}{2}}(1+k_1^2)^{\frac{1}{2}}- \\ Q_2'|k_1x-y-k_1x_1+y_1|[(x-x_2)^2+(y-y_2)^2]^{\frac{3}{2}}(1+k_2^2)^{\frac{1}{2}}=0 \\ Q_1'|k_3x-y-k_3x_3+y_3|[(x-x_1)^2+(y-y_1)^2]^{\frac{3}{2}}(1+k_1^2)^{\frac{1}{2}}- \\ Q_3'|k_1x-y-k_1x_1+y_1|[(x-x_3)^2+(y-y_3)^2]^{\frac{3}{2}}(1+k_3^2)^{\frac{1}{2}}=0 \end{cases} \tag{15}$$

The two unknowns, x and y, in the above nonlinear equations can be determined using the Newton-Raphson method [11-13]. Let $X=(x,y)^{\mathrm{T}}$ and $F(X)=(f_1,f_2)^{\mathrm{T}}$, where f_1 and f_2 represent the nonlinear equations of X described by (15), then X is solved iteratively using

$$X^{(n+1)}=X^{(n)}-F'(X^{(n)})^{-1}F(X^{(n)}) \tag{16}$$

where n=0, 1, …, and $F'(X)^{-1}$ is the inverse Jacobian matrix of $F(X)$.

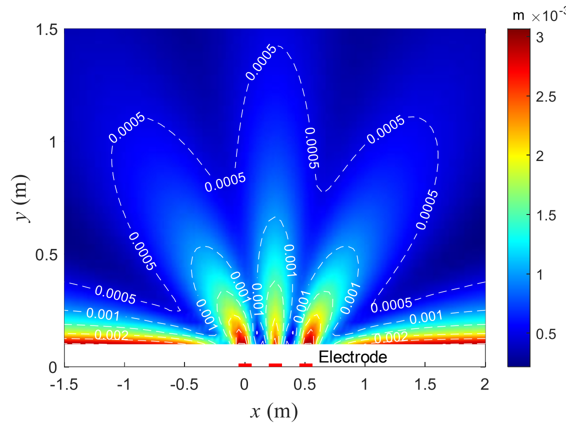

Fig. 4. Localization error of the linear sensor array.

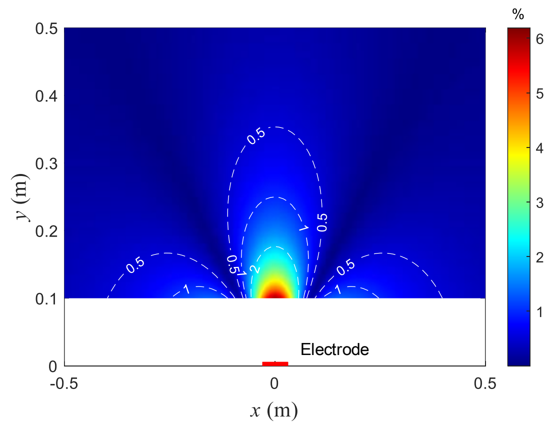

Fig. 5. Relative error of the induced charge calculated using equation (2) with reference to (17).

III. Results and Discussion

A. Simulation Method

The validity of the proposed localization method is verified via numerical simulation. Firstly, the forward problem is solved to find the induced charges on the electrodes for a point charge at a known location, which is termed as true location thereafter. Then, the inverse problem is solved to estimate the location of the point charge using the induced charges on the electrodes. Finally, the distance between the true and estimated locations are calculated for quantitative assessment of the localization error.

In the simulation, the electrode is square-shaped with a side length of 0.05 m. Instead of equation (2), equation (17) which is also derived using the method of images but makes no assumption of uniform electric field on the electrode surface is used to calculate more accurately the induced charges on the electrodes [14]

$$Q'=-\frac{Q}{\pi}\{\arctan[\frac{\frac{L}{2}(\frac{L}{2}-x)}{y\sqrt{(\frac{L}{2}-x)^2+\frac{L^2}{4}+y^2}})+\arctan(\frac{\frac{L}{2}(\frac{L}{2}+x)}{y\sqrt{(\frac{L}{2}+x)^2+\frac{L^2}{4}+y^2}}]\} \tag{17}$$

where L is the side length of an electrode located at the origin of the coordinate system. The quantity of the point charge Q is

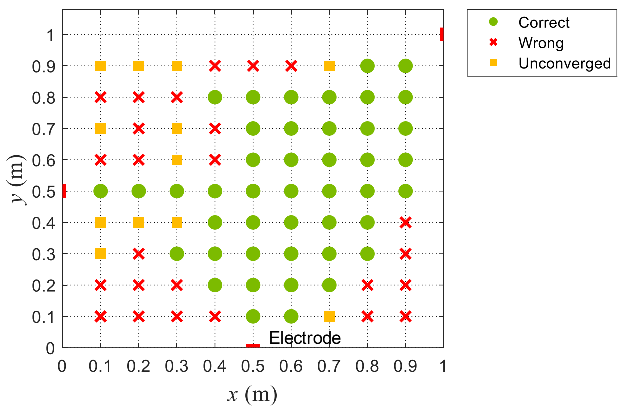

Fig. 6. Localization results of the three randomly positioned sensors.

arbitrarily set.

B. Results of the Linear Sensor Array

For assessment of the analytical solution for the linear sensor array, three electrostatic sensors are located at (0, 0), (0.25, 0) and (0.5, 0), respectively. The point charge is moved incrementally from -1.5 to 2.0 along the *x*-axis and from 0.1 to 1.5 along the *y*-axis. Fig. 4 shows the localization error in the vicinity of the sensor array. It can be seen that the localization error is basically below 0.003 m over the area under examination. The localization error increases when the point charge moves to the electrodes and the grounded surface. This arises from the increased error of the induced charge calculated using equation (2) with reference to (17), as illusrated in Fig. 5. As the point charge is close to the electrode and the grounded surface, the assumption of uniform electric field on the electrode surface does not hold anymore and the relative error of the induced charge can be significant.

C. Results of Three Randomly Positioned Sensors

To evaluate the numerical solution to the localization problem, three electrostatic sensors are located at (0.5, 0), (1.0, 1.0) and (0, 0.5) with the slopes of the grounded surfaces being 0, +∞, and +∞, respectively. Both the *x* and *y* coordinates of the point charge are incremented from 0.1 to 0.9 with a step of 0.1. Fig. 6 shows the localization results when the initial value of the iteration is set to (0.5, 0.5), which is the middle point of the investigated area. The results are labelled into three categories, namely Correct, Wrong and Unconverged. Correct results are those with a localization error smaller than 0.01 m, Wrong results are usually associated with a localization error much larger than 0.01 m, and Unconverged results mean that the solver does not converge within 30 iterations. It can be seen from Fig. 6 that Correct results are mostly located around the initial value, while Wrong and Unconverged results are close to the corners of the area.

More simulations have found that the localization results are highly dependent on the initial value. Wrong results are attributed to the non-uniqueness of the solution, which means that the relative magnitudes of the induced charges on the three electrodes at the true and estimated locations are almost the same. Some of the Wrong results are outside the investigated area and can be easily identified and removed. When Wrong or Unconverged results are obtained, a different initial value should be tried.

As discussed in [12], the need for an initial guess to start the solution process is a weakness of the Newton-Raphson method. However, it is possible to make a reasonable initial guess by fully exploiting the sensor data. For example, if the induced charge from the 1st electrode is obviously larger than those from the 2nd and 3rd electrodes, the initial value should be closer to the 1st electrode. The idea has been used in reference [13] where the initial value was obtained by averaging the TOF (time of flight) of three acoustic sensors for target localization. However, the determination of the initial value for localization using electrostatic sensors is more challenging because the induced change depends not only on the distance but also on the bearing of the charged object relative to the electrode. Additionally, there exist several modified Newton–Raphson methods with improved global convergence performance [15-17], which will be investigated in future. Other iterative methods such as Gauss–Newton and steepest descent methods as well as global exploration techniques such as the genetic algorithm and particle swarm optimization are also available for the root-finding problem [18].

D. Discussion

The localization method presented above is formulated using the method of image charges. It is critical that the electrodes are embedded in a large grounded surface in practice for the methods to be valid. Randomly positioned sensors enjoy greater deployment flexibility, but the linear sensor array should be preferred in order to avoid wrong and non-convergent results. More than three electrodes could be used to increase the localization accuracy by fusing the results of different combinations of the electrodes. Finally, extension to localization of charged objects in the three-dimensional space using the numerical method with at least four electrostatic sensors is straightforward.

IV. Conclusion

In this paper, localization of a charged object using electrostatic sensors in a plane has been presented. An analytical solution for a linear sensor array and a numerical solution for three randomly positioned sensors have been formulated. Numerical simulations have shown that the localization error increases as the point charge approaches the linear sensor array and the grounded surface. Depending on the initial value, the numerical solution could produce large localization errors and may not converge.

Experimental validation of the localization method under well-controlled conditions will be conducted in future work. For applications of the method in real scenarios, a variety of influencing factors such as medium heterogeneity, dimensions of the charged object and probing distance of the electrostatic sensor will be investigated and modifications to the method will be proposed to solve real-world localization problems.

REFERENCES

[1] Y. Yan, Y. Hu, L. Wang, X. Qian, W. Zhang, K. Reda, J. Wu, Ge Zheng. Electrostatic sensors - their principles and applications. Measurement, vol. 169, Art. no. 108506, 2021.

[2] F. Alam, N. Faulkner, B. Parr. Device-free localization: A review of non-RF techniques for unobtrusive indoor positioning. IEEE Internet of Things Journal, vol. 8, no. 6, pp. 4228-4249, 2020.

[3] H. Trinks, J. L. Ter Haseborg. Electric field detection and ranging of aircraft. IEEE Transactions on Aerospace and Electronic Systems, vol. AES-18, no. 3, pp. 268-274, 1982.

[4] M. A. Noras, S. P. Ramsey, B. B. Rhoades. Projectile detection using quasi-electrostatic field sensor array. Journal of Electrostatics, vol. 71, pp. 220-223, 2013.

[5] T. Addabbo, A. Fort, M. Mugnaini, E. Panzardi, S. Rocchi, V. Vignoli. Multisensor electrostatic detection of moving charged particles. Proceedings of 2016 IEEE Sensors Applications Symposium, Catania, Italy, 20-22 April 2016, pp. 1-6.

[6] W. Zhang, P. Li, N. Zhou, C. Suo, W. Chen, Y. Wang, J. Zhao, Y. Li. Method for localization aerial target in AC electric field based on sensor circular array. Sensors, vol. 20, Art. no. 1585, 2020.

[7] M. Man, Y. Zhang, G. Ma, Z. Zhang, M. Wei. Indoor localization method of personnel movement based on non-contact electrostatic potential measurements. Sensors, vol. 22, Art. no. 4698, 2022.

[8] T. Grosse-Puppendahl, X. Dellangnol, C. Hatzfeld, B. Fu, M. Kupnik, A. Kuijper, M. R. Hastall, J. Scott, M. Gruteser. Platypus - indoor localization and identification through sensing electric potential changes in human bodies. Proceedings of the 14th Annual International Conference on Mobile Systems, Applications, and Services, Singapore, 26-30 June 2016, pp. 17-30.

[9] B. Fu, F. Kirchbuchner, J. von Wilmsdorff, T. Grosse-Puppendahl, A. Braun, A. Kuijper. Performing indoor localization with electric potential sensing. Journal of Ambient Intelligence and Humanized Computing, vol. 10, pp. 731-746, 2019.

[10] S. N. Murnane, R. N. Barnes, S. R. Woodhead, J. E. Amadi-Echendu. Electrostatic modelling and measurement of airborne particle concentration. IEEE Transactions on Instrumentation and Measurement, vol. 45, no. 2, pp. 488-492, 1996.

[11] T. Sauer. Numerical analysis, 2nd ed., Pearson Press, 2011.

[12] W. H. Foy. Position-location solutions by Taylor-series estimation. IEEE Transactions on Aerospace and Electronic Systems, vol. AES-12, no. 2, pp. 187-194, 1976.

[13] N. Thong-un, S. Hirata, M. K. Kurosawa. Three-dimensional-positioning based on echolocation using a simple iterative method. International Journal of Electronics and Communications (AEU), vol. 69, pp. 680-684, 2015.

[14] Y. Hu, Y. Yan, Y. Yang. A comparative study of the preamplifiers in electrostatic sensors through analytical modeling and experimental evaluation. IEEE Transactions on Instrumentation and Measurement, vol. 71, Art. no. 2004610, 2022.

[15] L. Rao, R. He, Y. Wang, W. Yan, J. Bai, and D. Ye. An efficient improvement of modified Newton-Raphson algorithm for electrical impedance tomography. IEEE Transactions on Magnetics, vol. 35, no. 3, pp. 1562-1565, 1999.

[16] K. Hu, X. Song, Z. Sun, H. Luo, Z. Guo. Packet corruption tolerant localization for underwater acoustic sensor networks. Proceedings of 2020 IEEE Wireless Communications and Networking Conference, Seoul, Korea, 25-28 May 2020.

[17] F. Casella, B. Bachmann. On the choice of initial guesses for the Newton-Raphson algorithm. Applied Mathematics and Computation, vol. 398, Art. no. 125991, 2021.

[18] H. C. So. Source localization: Algorithms and analysis. in Handbook of Position Location: Theory, Practice, and Advances. John Wiley & Sons, Inc., New Jersey, 2011.